Int J Thermophys (2008) 29:312–321
DOI 10.1007/s10765-007-0340-6

Development of a New InGaAs Radiation Thermometer at NMIJ

Fumihiro Sakuma · Laina Ma · Tadashi Kobayashi

Published online: 11 January 2008

Abstract The first InGaAs radiation thermometer at NMIJ was developed more than ten years ago as a standard radiation thermometer operating from 150 to 1, 100°C. Its size-of-source effect (SSE) was as large as 1% from 6 mm in diameter to 50 mm in diameter. The new thermometer has an SSE of 0.3%. The reason for the error in measuring the SSE of InGaAs thermometers was also found. The new thermometer at first suffered from nonlinearity and the distance effect (DE). These deficiencies arose from the misalignment of optics inside the thermometer and were solved by increasing the detector size from 1 mm in diameter to 2 mm in diameter. Unfortunately, the detector of 2 mm diameter had a smaller S/N ratio than that of the 1 mm one at the indium (In) point. The final design uses a detector of 1 mm diameter, but the radiation is focussed on a smaller area of the detector. The new thermometer is smaller and lighter than preceding designs and other standard InGaAs radiation thermometers. The temperature of the main part of the instrument, including the filter, the detector, and the preamplifier board, is controlled at 30°C. In addition to the calibration with the six fixed points of copper (Cu), silver (Ag), aluminum (Al), zinc (Zn), tin (Sn), and indium (In), the linearity from the In point to the Cu point, the SSE, the DE, and the spectral responsivity were measured.

Keywords Calibration · Fixed-point blackbody · InGaAs · Linearity · Radiation thermometer · Size-of-source effect

F. Sakuma (✉) · L. Ma
National Metrology Institute of Japan (NMIJ), AIST, AIST Tsukuba Central 3, 1-1-1 Umezono, Tsukuba, Ibaraki 305-8563, Japan
e-mail: f-sakuma@aist.go.jp

T. Kobayashi
Chino Corporation, Tokyo, Japan

1 Introduction

InGaAs radiation thermometers are used as standard thermometers from 150 to 1, 000°C [1–5]. Some of them are used to check and compare standard blackbodies, and others are calibrated against fixed-point blackbodies to make a temperature scale by the multi-fixed-point method [6]. At NMIJ, an InGaAs radiation thermometer was developed ten years ago [2] that showed good quality, but the size-of-source effect (SSE) was a problem. The SSE between diameters of 6 and 50 mm changed as much as 1%. Recently, NMIJ and Chino jointly developed 0.65 and 0.9 μm standard radiation thermometers with a better SSE than the Topcon design [7]. The multiple reflections among lenses were simulated by using a ray-tracing technique to understand and suppress the SSE. This technique was applied to the InGaAs thermometer development. We evaluated the quality of the new thermometer in terms of the SSE, the distance effect (DE), the nonlinearity, the signal level at the indium point, and the spectral response characteristics. The problems we encountered, the countermeasures, and the results are described below.

2 Measurements

2.1 Radiation Thermometer

Several InGaAs thermometers were manufactured by Chino. The first one, IR-RST-16A, was manufactured in 1996 and was revised in 1997. The new InGaAs thermometer, IR-RST 16H, was manufactured in May 2006 (16p), revised in September (16 m), and revised again in November 2006 (16 H). The specifications of the new InGaAs thermometer are shown in Table 1. The temperature range is from 150 to 1, 100°C. The target size of 3 mm diameter at a measuring distance of 400 mm enables its calibration by fixed-point blackbodies having an aperture diameter of 6 mm [8]. The InGaAs detectors were made by Hamamatsu Photonics and are 1 or 2 mm in diameter. The temperatures of the detector and the interference filter are controlled at 30°C. The drawing of the IR-RST 16H is shown in Fig. 1. The length, width, and height are 290, 115, and 128 mm, respectively. The mass is about 3 kg. It is smaller and lighter than preceding designs and other standard InGaAs radiation thermometers. The optics of the new InGaAs thermometer are shown in Fig. 2. The objective lens positions and curvatures were designed with the ray-tracing technique so that the reflected light at each surface of the lenses does not reach the detector from multiple reflections among the elements. The objective lens was composed of three elements. The first two lenses form a doublet which is separated by as much as 64 mm, more than 70% of the objective focal length, from the third lens.

2.2 Testing

2.2.1 Size-of-Source Effect

The radiation source for the size-of-source measurements was an integrating sphere 400 mm in diameter with a barium-sulfate-coated inner wall and with six halogen

Table 1 Specifications of new InGaAs radiation thermometer

Item	Specifications
Temperature range	150–1, 100°C
Temperature resolution	Better than 0.1°C at 160°C
Stability	Better than 0.1°C at 160°C
Interference filter	
Center wavelength	1.6 μm
Full width at half maximum	0.15–0.20 μm
Out of band suppression	Less than 10^{-4}
Measuring distance	400 mm to infinity
Minimum target size	ϕ3 mm
Size-of-source effect	Less than 1% for 6–140 mm diameter
Optics	Lens system
Finder	With a reticule
Detector	InGaAs photodiode
Detector temperature	
Setting temperature	30°C
Stability	±0.1°C
Amplifier	Field-effect transistor input operational amplifier
Feedback resistance	Three stages: 100 MΩ, 3 MΩ, 100 kΩ
Output signal	DC signal 0–10 V
Output stability	Better than ±0.1 mV
Linearity	Better than ±0.05%

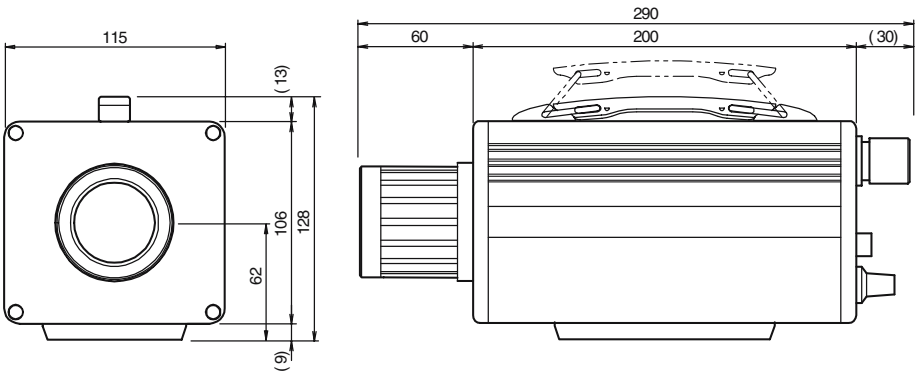

Fig. 1 Drawing of InGaAs radiation thermometer IR-RST-16H

lamps inside. The sphere has an exit port 140 mm in diameter. A quartz plate with a black spot and an aperture plate were placed at the exit. Black spots and apertures of various sizes were used to obtain the diameter dependence of the SSE. The ratio between the output signals in observing the black spot and the bright area is the SSE.

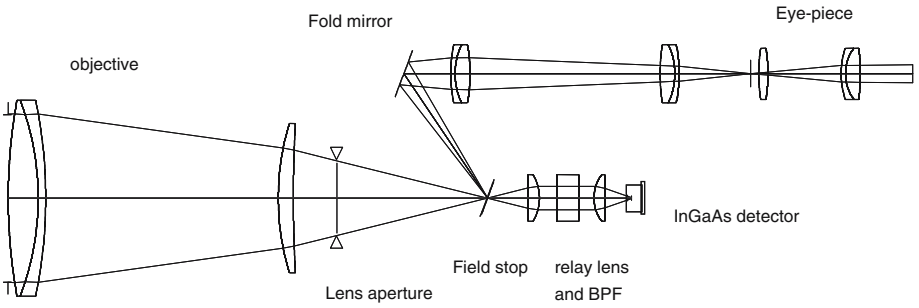

Fig. 2 Optics of InGaAs radiation thermometer IR-RST-16 H

2.2.2 Distance Effect

An integrating sphere 250 mm in diameter was used as the radiation source. The sphere was mounted on a translation stage 800 mm in length to change the measuring distance. At each measuring distance, the thermometer focus was adjusted.

2.2.3 Nonlinearity

The two-aperture method was used for the nonlinearity measurement. A rotating disk opened and closed two apertures independently. An integrating sphere and a halogen lamp were used as radiation sources for low radiance and high radiance, respectively.

2.2.4 Fixed-Point Blackbodies

Indium (In, 156.5985°C), tin (Sn, 231.928°C), zinc (Zn, 419.527°C), aluminum (Al, 660.323°C), silver (Ag, 961.78°C), and copper (Cu, 1084.62°C) were used as the fixed points. Each fixed-point blackbody has an aperture of 6 mm diameter and an effective emissivity estimated as 0.999 [8] and 0.9995 for the outer aperture and inner aperture, respectively.

2.2.5 Spectral Responsivity

A double-grating monochromator 250 mm in focal length covered a spectral range from 400 to 2,500 nm. Two sets of gratings were used; one had 1,200 lines/mm with a 750 nm blaze and the other had 300 lines/mm with a 1,600 nm blaze. A mercury lamp was used to calibrate the wavelength scale of the monochromator.

3 Results

3.1 Size-of-source Effect

Figure 3 shows the SSE results of the 16 A and 16 H thermometers denoted by an open square and a closed diamond, respectively. The reference diameter is 6 mm. The SSE

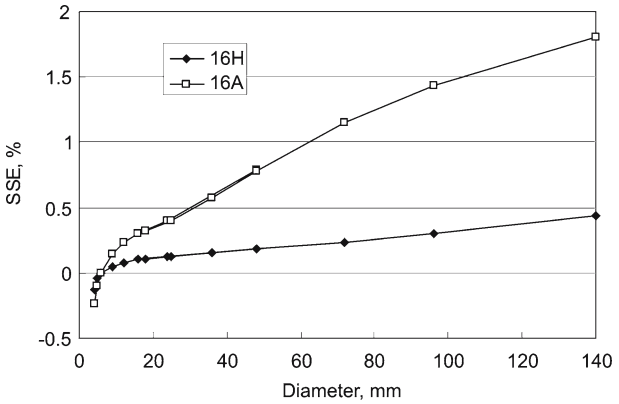

Fig. 3 Size-of-source effect (SSE) of InGaAs radiation thermometer

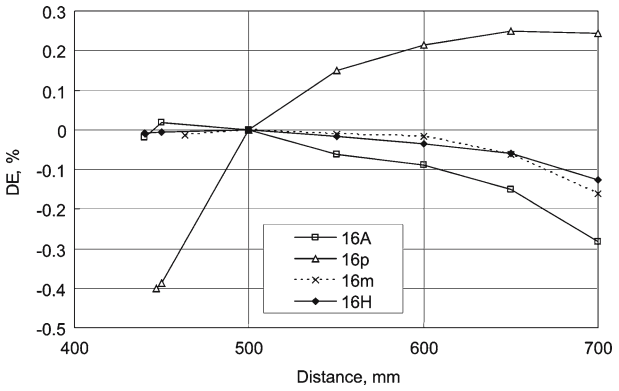

Fig. 4 Distance effect (DE) of InGaAs radiation thermometer

of the 16 A was 1% at 50 mm diameter while that of the 16 H was 0.2%. The SSE values were almost the same among 16 p, 16 m, and 16 H.

3.2 Distance Effect

Figure 4 shows the DE results of the four thermometers. The DE of the 16p was large and amounted to 0.65% between the distances of 450 and 700 mm. The DE of the 16 m and 16 H were half as large as that of the 16 A and much smaller than the SSE.

3.3 Nonlinearity

Figure 5 shows the nonlinearity of the 16 p, 16 m, and 16 H. The ordinate *NL* shows the nonlinearity at the radiance doubling. The outputs when both apertures A and B are open, only A is open, only B is open, and both are closed are denoted by V_{AB}, V_A,

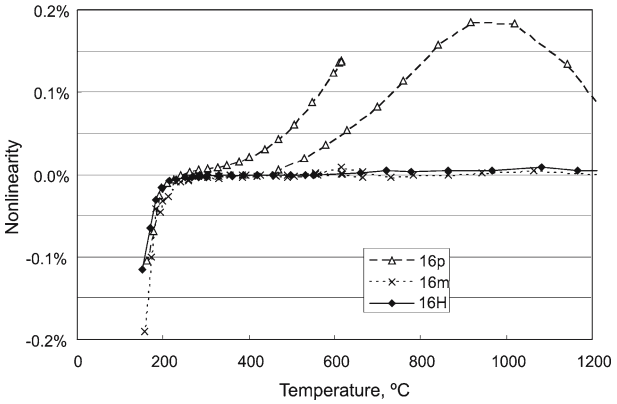

Fig. 5 Nonlinearity of InGaAs radiation thermometer. In the abscissa, the output V_{AB} was converted to temperature by Eq. 2

V_{B}, and V_{Zero}, respectively. The nonlinearity NL is expressed as follows:

$$NL = \frac{V_{\mathrm{AB}} + V_{\mathrm{Zero}} - V_{\mathrm{A}} - V_{\mathrm{B}}}{V_{\mathrm{AB}} - V_{\mathrm{Zero}}} \tag{1}$$

A large 'super linearity' of about +0.2% was observed for the 16p around 1,000°C, which corresponds to a photocurrent of about 30 μ A. When the incident radiance is doubled, the output signal increases by more than twice its initial value. At temperatures below 200°C, or a photocurrent below 0.2 nA, the three thermometers were found to deviate from linear behavior.

3.4 Fixed-point Calibration

Six fixed-point blackbodies were used to calibrate the thermometers. Figure 6 shows the freezing curve of the indium point. The noise level was worse for 16 m, which has a larger detector diameter than the others. The 16 H was the best among the four, with a standard deviation of 10 mK. The six calibration data points were used to fit the interpolation equation,

$$V(T) = \frac{C}{\exp(\frac{c_2}{AT+B}) - 1}, \tag{2}$$

where c_2 is the second radiation constant and A, B, and C are the coefficients of the thermometer determined from the fitting procedure. The residuals at the fixed points were less than ± 32 mK.

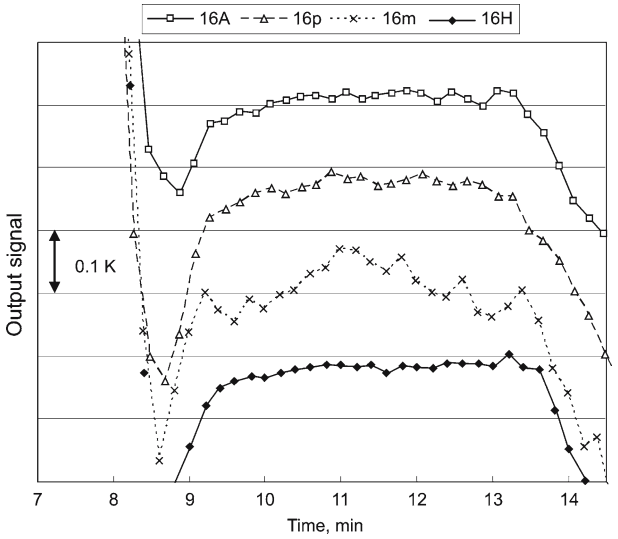

Fig. 6 Freezing curve of indium point measured by InGaAs radiation thermometer. The ordinate of each curve has an offset to show each profile clearly

3.5 Spectral Responsivity

Figure 7 shows the spectral responsivity of the 16 H (solid line) and the 16 A (broken line). Figure 7a shows the linear ordinate in the central part, and Fig. 7b shows the logarithmic ordinate over a wide range. The center wavelengths of the 16 H and the 16 A were 1594.4 and 1598.8 nm, respectively. Their bandwidths were about 142 nm. The linear profiles in Fig. 7a are almost the same, but the logarithmic profiles in Fig. 7b show differences. The shoulders of the 16 H were much sharper than those of the 16 A. The relative responsivities of the 16 H at 1,400 and 1,800 nm were two orders of magnitude smaller than those of the 16 A.

4 Discussion

4.1 Size-of-source Effect

By employing a new optical design for the objective lens, the SSE of the new InGaAs thermometers was much improved compared to the preceding design. The SSE value of 0.2% for the 16 H thermometer is almost the same as in [3] and [4], but is larger than the values in [5] and [9]. Considering the small size of the 16 H, this SSE value is allowable and measurements can be corrected by using the testing curve of Fig. 3.

While measuring the SSE, we found that the black spot was not really black at 1.6 μm. The transmittance was less than 0.001% at 0.9 μm, but it increased to 0.05% at 1.6 μm [10]. The difference found in the two methods of measuring the SSE [11] might be caused by this transmittance. We corrected the transmittance in our SSE

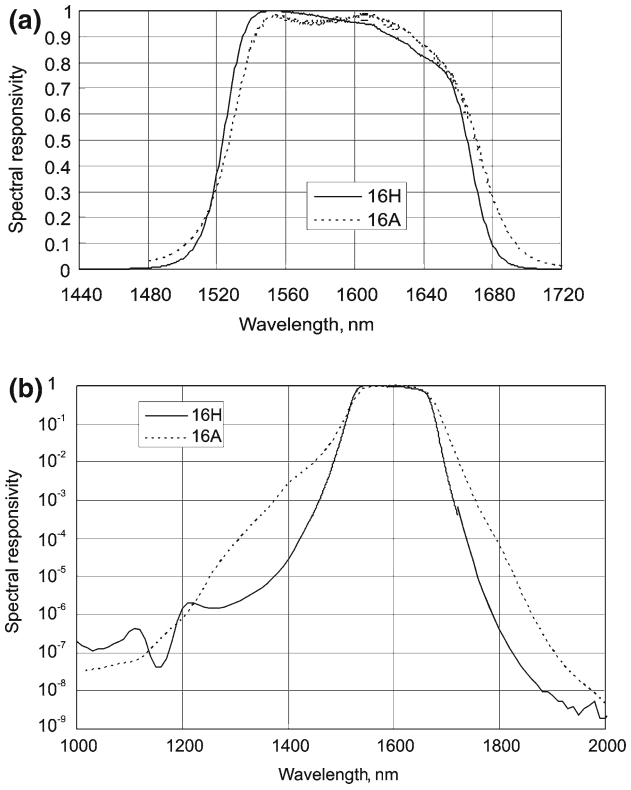

Fig. 7 Spectral responsivity of InGaAs radiation thermometer

measurements. This correction provided better agreement of the SSE results between the aperture size change and the black-spot size change.

4.2 Misalignment

The cause of the large DE in Sect. 3.2 and the large nonlinearity in Sect. 3.3 of the 16p thermometer were found to be due to misalignment of the optics in the thermometer. The position of the aperture was a little off-center, and the focused light hit the edge of the detector, as found in [9]. The first attempt at correction was to use a larger detector to receive all the focused light. We changed the detector diameter from 1 to 2 mm. Then, the large nonlinearity disappeared and the DE became normal. However, the 2 mm detector exhibited greater noise at the In freezing point (Fig. 6). Therefore, the final solution was to use a 1 mm detector, to make a smaller image of the target on the detector to avoid edge effects, and to adjust the position of the aperture precisely by using a newly made jig. The output of the final version 16 H was as large as the 16 m with the 2 mm detector.

4.3 Nonlinearity

The output signal of the InGaAs thermometer changes more than 10^6 times from the In point to the Cu point. Therefore, the nonlinearity check is important for use of the thermometer. Although the high-temperature nonlinearity of the 16p was suppressed by adjusting the alignment, the low-temperature nonlinearity still existed. This nonlinearity became noticeable below the tin point. This effect was not from the amplifier because the same output signals for other ranges did not show this nonlinearity. The effect amounted to 0.1% at the indium point, corresponding to 0.02°C. The nonlinearity made the measured output at the In point larger than the calculated output estimated from higher temperatures. The cause of the nonlinearity might be that the feedback resistance was larger than the shunt resistance.

4.4 Spectral Response

To avoid the absorption bands of water and carbon dioxide located at 1.4 μm and to have enough bandwidth, the center wavelength and the bandwidth of the InGaAs thermometer were selected as 1.6 μm and 150 nm, respectively. The noise level of the InGaAs detector would be smaller if the detector temperature was cooled. However, the spectral response at longer wavelengths would decrease upon cooling to lower temperatures. Therefore, the detector temperature was maintained at 30°C. The new thermometer 16 H has much smaller responsivity at 1.4 μm, so the humidity influence on the 16 H is less than that of the 16 A.

To check the scale realization, an independent scale was realized by integrating the spectral responsivity $R(\lambda)$ multiplied by the Planck function $L(\lambda, T)$,

$$V(T) = a \int L(\lambda, T) R(\lambda) \mathrm{d}\lambda. \tag{3}$$

Table 2 Evaluation of InGaAs radiation thermometer

	16 A	16p	16 m	16 H
Manufacture/revision	1997	May 2006	September 2006	November 2006
Detector	G5832-11	G8560-01	G5832-02	G8560-01
Diameter	1 mm	1 mm	2 mm	1 mm
Shunt resistance at 30°C	70 MΩ	70 MΩ	22 MΩ	70 MΩ
SSE (6–50 mm)	1%	0.2%	0.2%	0.2%
DE (450–700 mm)	−0.3%	0.6%	−0.18%	−0.12%
Nonlinearity at 1, 000°C	0.0%	0.2%	0.0%	0.0%
Noise level at In point (2σ)	16 mK	15 mK	57 mK	10 mK
Spectral responsivity	Good	–	–	Sharper
Note	Large SSE	Misalignment	Low S/N	Good

Here, the coefficient a was determined from the copper-point calibration. The differences of the five fixed-point measurements from the integration scale were less than ±0.15°C.

5 Conclusions

Table 2 summarizes our evaluation of the various thermometers. The new InGaAs radiation thermometer IR-RST 16 H was developed as a standard radiation thermometer from 150 to 1, 100°C. The estimated characteristics of the SSE, the DE, the S/N ratio, and the spectral responsivity were better than the old IR-RST-16 A.This thermometer 16 H is compact and easy to operate, and therefore it will be used to establish the traceability of low-temperature radiation thermometers.

References

1. T. Ricolfi, M. Battuello, in *Temperature: Its Measurement and Control in Science and Industry*, vol. 6, Part 2, ed. by J.F. Schooley (AIP, New York, 1992), pp. 797–800
2. F. Sakuma, J. Ishii, M. Kobayashi, in *TEMPBEIJING '97: Proceedings of the International Conference of the Temperature and Thermal Measurements*, ed. by B. Zhang, L. Han, X. Zhao (Standards Press of China, Beijing, 1997), pp. 78–83
3. B. Gutschwager, J. Fischer, in *Proceedings of TEMPMEKO '99, 7th International Symposium on Temperature and Thermal Measurements in Industry and Science*, ed. by J. F. Dubbeldam, M. J. de Groot (Edauw Johannissen bv, Delft, 1999), pp. 567–572
4. B. Chu, H. McEvoy, G. Machin, in *Temperature, Its Measurement and Control in Science and Industry*, vol. 7, Part 2, ed. by D.C. Ripple (AIP, New York, 2003), pp. 571–576
5. E. Schreiber, G. Neuer, in *Proceedings of TEMPMEKO 2004, 9th International Symposium on Temperature and Thermal Measurements in Industry and Science*, ed. by D. Zvizdić, L.G. Bermanec, T. Veliki, T. Stašić (FSB/LPM, Zagreb, Croatia, 2004), pp. 527–532
6. F. Sakuma, S. Hattori, in *Temperature, Its Measurement and Control in Science and Industry*, vol. 5, Part 1, ed. by J.F. Schooley (AIP, New York, 1982), pp. 421–427
7. F. Sakuma, L. Ma, T. Suzuki, T. Kobayashi, A. Nakanishi, H. Katayama, *Proceedings of SICE* 2004 (Sapporo, 2004), FPI-4-2, pp. 72–76
8. F. Sakuma, S. Hattori, in *Temperature, Its Measurement and Control in Science and Industry*, vol. 5, Part 1, ed. by J.F. Schooley (AIP, New York, 1982), pp. 535–539
9. M. Battuello, F. Girard, T. Ricolfi, in *Proceedings of TEMPMEKO 2004, 9th International Symposium on Temperature and Thermal Measurements in Industry and Science*, ed. by D. Zvizdić, L.G. Bermanec, T. Veliki, T. Stašić (FSB/LPM, Zagreb, Croatia, 2004), pp. 505–508
10. L. Ma, F. Sakuma, *Proceedings of SICE* 2007 (Takamatsu, 2007), pp. 1743–1747
11. G. Machin, R. Sergienko, in *Proceedings of TEMPMEKO 2001, 8th International Symposium on Temperature and Thermal Measurements in Industry and Science*, ed. by B. Fellmuth, J. Seidel, G. Scholz (VDE Verlag, Berlin, 2002), pp. 155–160